Statistical analysis

Results are presented as the mean ± SD. Statistical analysis was performed using Student's t-test and one-way analysis of variance (ANOVA). A p-value of less than 0.05 was considered to be statistically significant.

Ethical considerations

This experiment was reviewed by the Committee of Animal Experiment Ethics in Yamaguchi University School of Medicine and was carried out under the Guidelines for Animal Experiments in Yamaguchi University School of Medicine (No. 105) and Notification (No. 6) of the Japanese Government.

Results

Effects of TJ-9 on MMP-2, 13 and TIMP-1 mRNA expression of activated HSC

Messenger RNA expression was investigated by Northern blot analysis on day 4 after culture. Under control culture conditions (no treatment), HSCs expressed MMP-2, 13 and TIMP-1 mRNAs (Fig. 1A, 1B, lane 1). 500 μg/ml of TJ-9 significantly elevated MMP-2 transcripts expressed at 3.1 kb and strikingly inhibited TIMP-1 mRNA expression (Fig. 1A, 1B, line 2). Expression of MMP-13 mRNA with stellate cells was dramatically reduced in a time-dependent manner after isolation. Although MMP-13 mRNA expression was not detected after 4-day culture, addition of 500 μg/ml of TJ-9 increased MMP-13 mRNA expression to a detectable level, though it was still very weak (Fig. 1A, 1B). Reduction of type I procollagen mRNA expression could be reproduced with 500 μg/ml of TJ-9 as previously reported (Kayano et al., 1998).

Morphologically, TJ-9 seemed to prevent the transformation to myofibroblast-like cells as previously reported (data not shown) (Kayano et al., 1998).

The doses up to 1000 μg/ml of TJ-9 showed no cytotoxicity with cultured stellate cells.

Effects of TJ-9 on MMP-2 and TIMPs production by activated HSC

When serum-free conditioned media derived from HSCs were analyzed on polyacrylamide gels co-polymerized with 1 mg/ml gelatin, the band of lysis was observed in the zymograms. These gelatinolytic activities were completely inhibited when the gels were incubated in the presence of 20mM EDTA (data not shown), indicating that they were mediated by metalloproteinases. TJ-9 conditioned media exhibited gelatinase activities in a dose-dependent manner on gelatin zymograms, seen mainly as a triplet with bands at molecular masses of 70, 66 and 62kDa (Fig. 2A). The 66 kDa gelatinase predominanted, and the 62 kDa band was at the limit of detection. These bands migrated in the Mr 62-70 kDa region corresponding to the predicted molecular weights for MMP-2. The appearance of these bands was dependent on the concentration of TJ-9, and gelatinase activity reached a peak at the concentration of 500 or 1000 μg/ml. Upregulation of MMP-2 production was also confirmed by quantitative measurement using the type IV collagen-degrading assay. Collagen IV

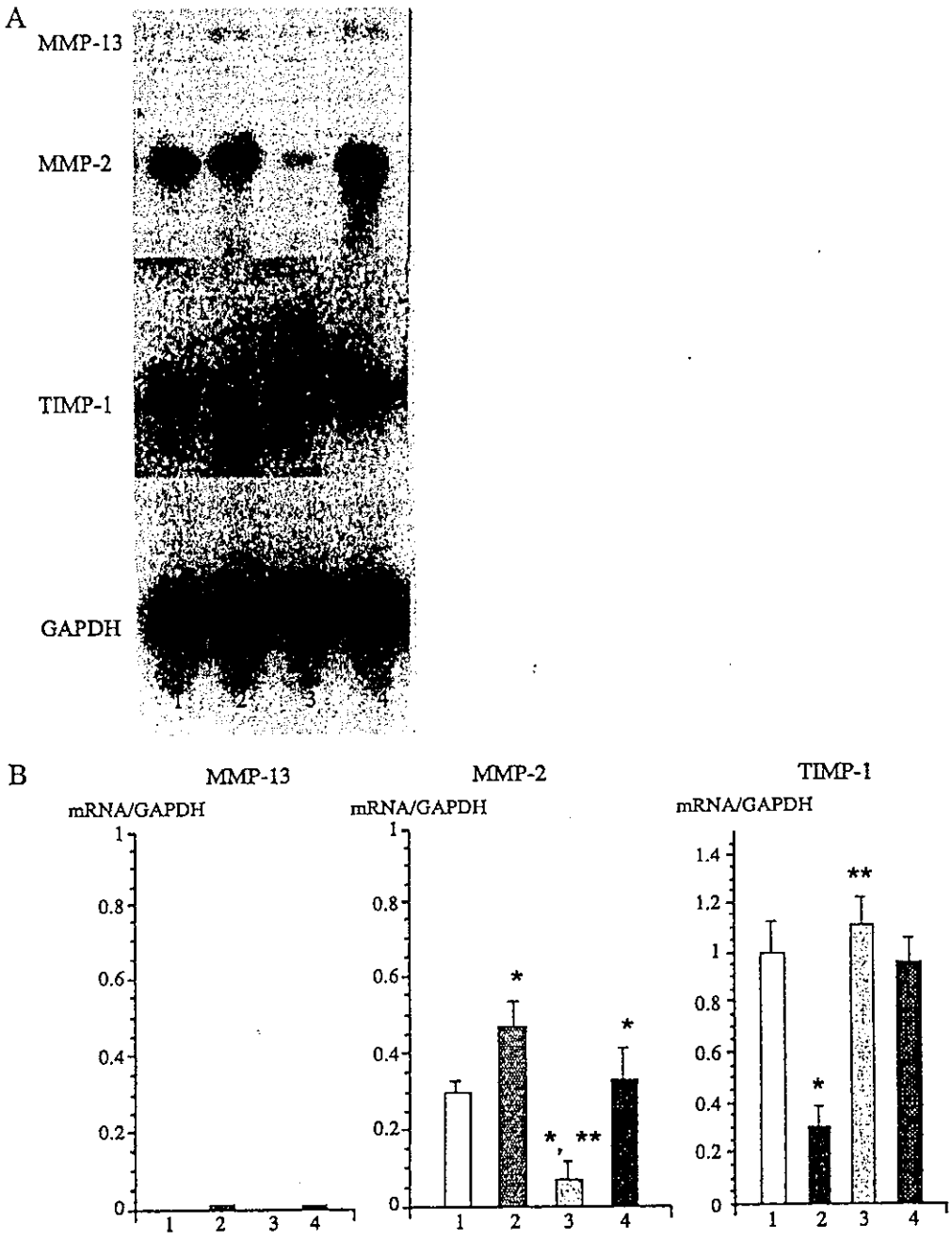

Fig. 1. A. Messenger RNA expression of MMP-13, MMP-2, TIMP-1 and G3PDH. Freshly isolated hepatic stellate cells were cultured for 4 h. The medium was replaced without TJ-9 (lane 1), with 500 μg/ml TJ-9 (lane 2), with 500 μg/ml TJ-9 plus 10 μM SB203580 (lane 3) and with 500 μg/ml TJ-9 plus 50 μM PD 98059 (lane 4). The medium was changed every 24 h. After 4 days, mRNA expression was examined. The figure shows a representative example of 5 independent Northern blots. B. Graphic representation of Fig. 1. The results of the densitometric analysis after normalization against hybridization signals for G3PDH are shown mean ± SD of 5 independent experiments. * $P<0.01$ vs lane 1 (control), ** $P<0.01$ vs lane 2 (TJ-9 500 μg/ml).

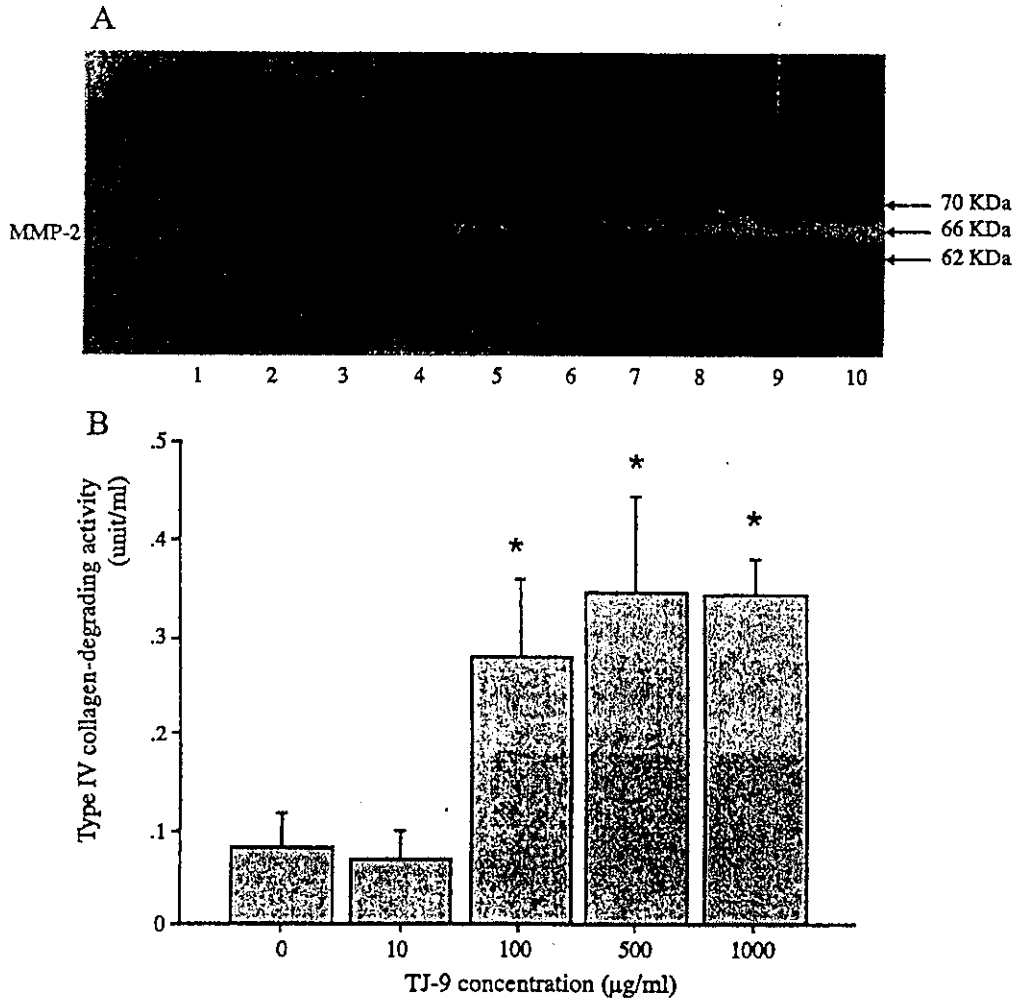

Fig. 2. A. Zymography with various concentrations of TJ-9. Freshly isolated hepatic stellate cells were cultured for 4 h. The medium was replaced without TJ-9 (lane 1, 2), or with 10 μg/ml (lanes 3, 4), 100 μg/ml (lanes 5, 6). 500 μg/ml (lanes 7, 8), and 1000 μg/ml (lanes 9, 10) of TJ-9. After 4 days, zymography was performed. B. Quantitative analysis of type IV collagen-degrading activity was done instead of zymography shown in Fig. 2-A. The results are shown as mean ± SD of 5 independent experiments. * $P<0.01$ vs 0 (control).

decomposition by serum-free conditioned media derived from HSCs increased dose-dependently and reached a peak at the concentration of 500 μg/ml of TJ-9, consistent with zymograms (Fig. 2B).

TJ-9 markedly reduced the activity of TIMPs from HSC in a dose-dependent manner as shown by a reverse zymogram (Fig. 3). This inhibitory effect on the activity of TIMP-1, 2 reached a peak at the concentration of 500 μg/ml of TJ-9. Thus, the TJ-9-enhanced gelatinolytic activity in culture media could be mainly attributed to the decreased synthesis of TIMPs in addition to the increased MMP-2 production.

Although the changes of MMP-2 or TIMP-1 mRNA expression were not remarkable, the treated cells showed prominent changes of activity, which is more physiologically relevant.

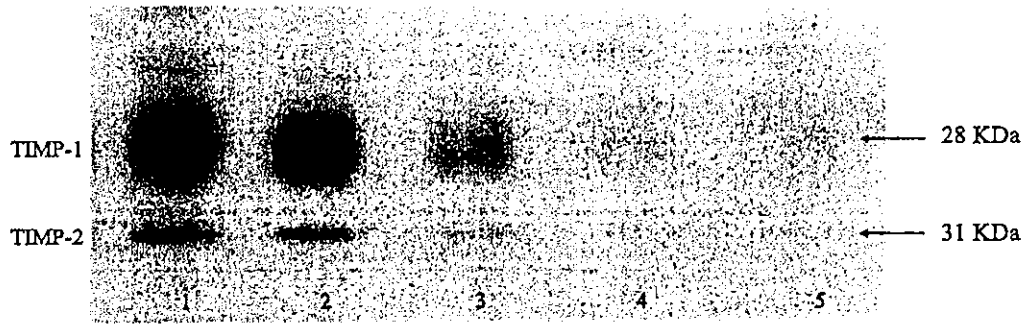

Fig. 3. Reverse zymography with concentrations of TJ-9. Freshly isolated hepatic stellate cells were cultured for 4 h. The medium was replaced without TJ-9 (lane 1), or with 10 μg/ml (lane 2), 100 μg/ml (lane 3). 500 μg/ml (lane 4), and 1000 μg/ml (lane 5) of TJ-9. After 4 days, reverse zymography was performed. The figure shows a representative example of 5 independent experiments. * $P < 0.01$ vs 0 (control).

Effect of inhibitors of MAPKs on expression of MMPs and TIMPs

The functional role of MAP kinases in mediating the down-regulatory effect of TJ-9 on expression of TIMPs and the up-regulatory effect on MMPs expression were examined.

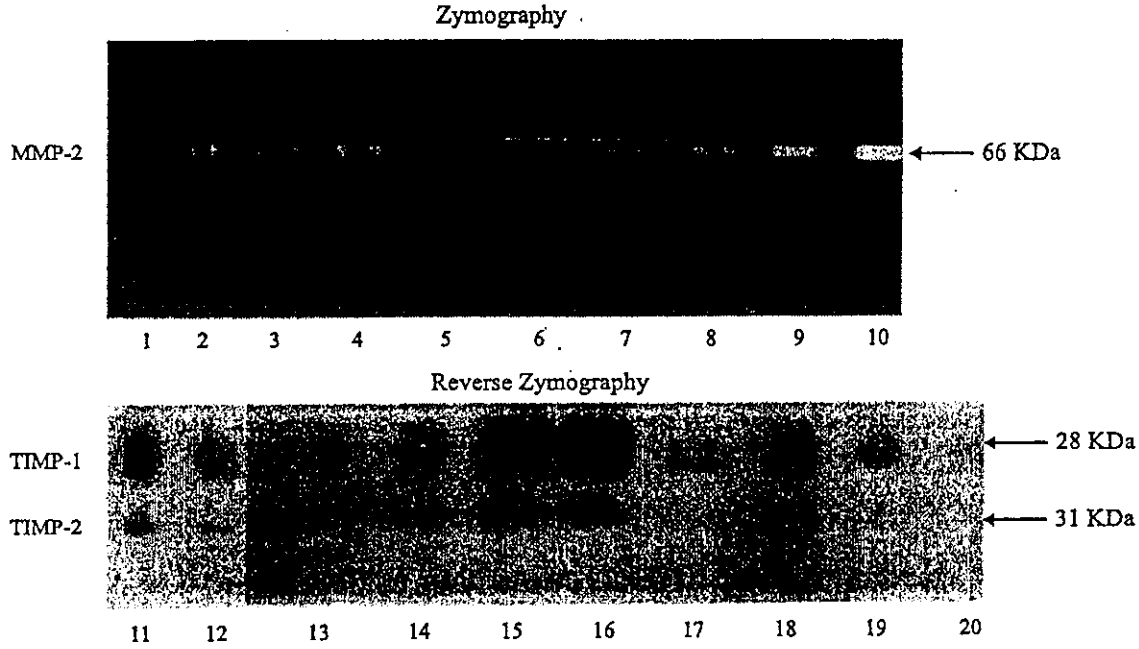

Fig. 4. Effects of SB203580 and PD98059 on MMP-2 and TIMP-1, 2 expression of TJ-9 treated hepatic stellate cells. Freshly isolated hepatic stellate cells were cultured for 4 h. The medium was replaced without TJ-9 (lanes 1, 11), with 500 μg/ml TJ-9 (lanes 2, 12), with 500 μg/ml TJ-9 plus 0.01 μM SB203580 (lanes 3, 13), with 500 μg/ml TJ-9 plus 0.1 μM SB203580 (lanes 4, 14) , with 500 μg/ml TJ-9 plus 1 μM SB203580 (lanes 5, 15) with 500 μg/ml TJ-9 plus 10 μM SB203580 (lanes 6, 16), with 500 μg/ml TJ-9 plus 0.05 μM PD98059 (lanes 7, 17), with 500 μg/ml TJ-9 plus 0.5 μM PD98059 (lanes 8, 18), with 500 μg/ml TJ-9 plus 5 μM PD98059 (lanes 9, 19), or with 500 μg/ml TJ-9 plus 50 μM PD98059 (lanes 10, 20). After 4 days, zymography and reverse zymography were performed.

The effect of SB203580 (Cuenda et al., 1995), a specific inhibitor of p38 MAP kinase activation, was examined.

The expression of MMP (MMP-13, MMP-2) mRNAs was significantly reduced (Fig. 1A, 1B [b, c], lane 3). On the other hand, the effect of TJ-9 on the expression of TIMP-1 mRNA was completely diminished by treatment of SB203580 (Fig. 1A, 1B [d], lane 3).

These results were confirmed by the zymogram and reverse zymogram shown in Fig. 4 (lanes 1-6, 11-16). SB203580 reduced the activity of MMP-2 (Fig. 5) and increased the activity of TIMP-1, 2 in a dose-dependent manner in TJ-9 treated HSCs.

To elucidate the role of the ERK pathway in the effects of TJ-9, HSCs were treated with various concentrations of PD98059, a specific inhibitor of MEK activation, which prevents activation of ERK

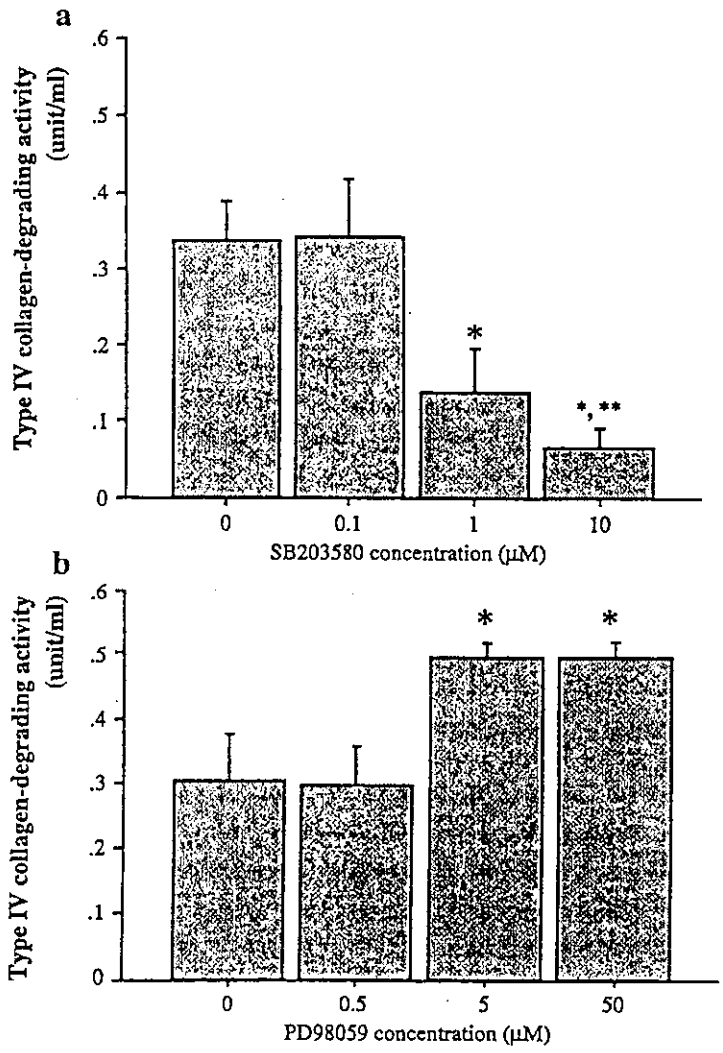

Fig. 5. Quantitative analysis of type IV collagen-degrading activity was done for the comparison of the zymography shown in Fig. 5. The results are shown as mean ± SD of 5 independent experiments. * $P<0.01$ vs 0 (control), ** $P<0.05$ vs 1 (SB203580 1 μM).

(Dudley et al., 1995). PD98059 had no noticeable effect on changes in mRNAs level but there was a mild increase in MMP-2 activity measured with zymogram (Fig. 4) and type IV collagen-degrading assay (Fig. 5).

Although SB20380 and PD980597 were dissolved in DMSO at the final concentration of 0.1%, 0.1% DMSO by itself had no effect on the activity of MMP-2 or TIMP-1, 2 (data not shown).

These results showed that the activity of p38 MAP kinase seemed to be essential to prevent TIMP-1, 2 expressions and enhance MMP-2 expression in TJ-9 treated HSCs.

Discussion

We have previously shown that TJ-9 prevents fibrosis by the inhibition of HSCs with reduced type I procollagen mRNA expression in different animal models of fibrosis due to choline-deficiency (Sakaida et at., 1998a,b), and pig serum (Shimizu et al., 1999). Also we have already reported that doses up to 1000 μg/ml of TJ-9 inhibit type I procollagen mRNA and the cell cycle of cultured stellate cell without any cytotoxicity (Kayano et al., 1998). In this study, we examined the effect of TJ-9 on the balance between MMP-2 and TIMP-1,2 with cultured HSCs.

First we showed that 500 μg/ml of TJ-9 markedly reduced TIMP-1 mRNA expression with enhanced mRNA expression of MMP-2. We choose this dose because 500 μg/ml of TJ-9 was most effective for the prevention of type I procollagen mRNA expression, as reported previously (Kayano et al., 1998). Then activity of MMP-2 and TIMPs was examined by zymogram or reverse zymogram. The reverse zymogram clearly indicated that TJ-9 reduced TIMP-1, 2 activities in a dose-dependent manner up to 500 μg/ml, with enhanced MMP-2 activity (Figs. 2, 3). The effect of TJ-9 on MMP-2 activity was also quantitatively examined by a type IV collagen degrading assay showing the peak value at the concentration of 500 μg/ml.

Secondary, the effects of TJ-9, i.e. the inhibition of TIMP-1 expression and induction of MMP-2 expression, were completely abolished by the selective p38 MAP kinase inhibitor SB203580 in a dose-dependent manner, indicating that p38 MAP kinase activity was essential for reduction of TIMP-1 expression and induction of MMP-2 expression.

In contrast, inhibition of the ERK pathway by PD98059, a selective inhibitor of MEK activation, caused only slight enhancement of MMP-2 activity without affecting mRNAs level in HSCs treated with TJ-9 (500 μg/ml).

Our findings are consistent with the recent works reporting that p38 MAP kinase may be closely related with the expression of MMP-2 in human endothelial cell (Lee et al., 2000) or the MMP-9 (Underwood et al., 2000; Simon et al., 1998) or the MMP-13 (Ravanti et al., 1999a,b) expression in different cells other than HSCs. Eberhardt W et al (Eberhardt et al., 2000) reported that IL-1β induced MMP-9 and TIMP-1 expressions in rat glomerular mesangial cells with increased activity of MPAKs cascades (ERK, SAPK/JNK and p38 MAP kinase) leading to increased activity of NF-κB and AP1 and Solis-Herruzo JA et al (Solis-Herruzo et al., 1999) also indicated that interleukin-6 induced MMP-13 and TIMP-1 expressions in rat fibroblast through stimulation of AP1. Both reports found that either MMP-9 or MMP-13 expression paralleled with the expression of TIMP-1.

It has been reported (Benyon et al., 1999)that activated hepatic stellate cells increase MMP-2 and TIMP-2 expression in a time-dependent manner on culture dishes until 7 days and that the increase in MMP-2 expression of stellate cells is responsible for degrading the normal basement

membrane, not type I collagen. Thus a question may be raised as to whether the increase in MMP-2 expression with TJ-9 treatment can be pro-fibrogenic in terms of stellate cell activation. However, TJ-9 also induced MMP-13 mRNA expression, which is responsible for degrading interstitial collagens, e.g. type I collagen. It is also known (Iredale et al., 1996) that enhanced TIMP-1,2 expresssion relative to interstitial collagenase (MMP-1/MMP-13) expression leads to the accumulation of collagens (fibrogenesis) and the reduction of TIMP-1,2 expression relative to interstitial collagenase (MMP-1/MMP-13) expression, even weak expression, can lead to the resolution of liver fibrosis (fibrolysis).

Kato et al. (Kato et al., 1998) previously reported opposite result. The treatment of melanoma cells with TJ-9 (400 μg/ml), a dose similar to that used here, showed the downregulation of MMP-2 and upregulation of TIMP-1. Studies of different cell types, e.g. malignant cells or benign cells, may reconcile these different results but further studies using other cells are necessary.

Current studies reported that an IL-10 associated silencer element (HTS) (5′ -CCACTGGCC-CATCGTATAT-3′) (-1284 to -1266 bp) in the 5′ promoter region of the TIMP-1 gene functions as a negative regulatory element that controls TIMP-1 expression (Wang et al., 1998) and upstream TIMP-1 element-1 (UTE-1) is essential for transcriptional activity of the human TIMP-1 promoter (Trim et al., 2000).

On the other hand, the promoter for the MMP-2 gene contains an AP-2 site and GC boxes (Benbow and Brinckerhoff, 1997). Chen et al. reported that MAP kinase pathways utilize a GC box to regulate gene transcription in rat HSC (Chen and Davis, 1999). It has also been reported that the MAP kinase signaling cascade stimulates Sp1 binding (Merchant et al., 1999).

But further examinations are necessary to clarify the exact relationships and cross-talk of MAPKs cascades in the expression of MMPs and TIMPs.

In conclusion, the results of this study show that TJ-9 treatment leading to upregulatation of MMP-2, 13 production and downregulation of TIMP-1,2 production. The manipulation of the balance of TIMPs and MMPs may provide new insights for the treatment of liver fibrosis.

Acknowledgements

This work was supported in part by Grants-in-Aid 11670507 and 13470121 from the Ministry of Education, Science and Culture, Japan.

References

Araki, N., Noda, T., Ogawa, K., 1988. Cytochemical studies on the effect of intraperitoneal and oral administration of a traditional Chinese medicine (Sho-saiko-to) on the D-galactosamine-induced hepatic injuries of rats. Acta Histochemia et Cytochemica 21, 439–453.

Benyon, R.C., Hovell, C.J., Da Gaca, M., Jones, E.H., Iredale, J.P., Arthur, M.J., 1999. Progelatinase A is produced and activated by rat hepatic stellate cells and promotes their proliferation. Hepatology 30, 977–986.

Boulton, T.G., Nye, S.H., Robins, D.J., Radziejewska, E., Morgenbesser, S.D., DePinho, R.A., Panayotatos, N., 1991. ERKs: a family of protein-serine/threonine kinases that are activated and tyrosine phosphorylated in response to insulin and NGF. Cell 65, 663–675.

Cohen, P., 1997. The search for physiological substrates of MAP and SAP kinases in mammalian cells. Trends Cell Biology 7, 353–361.

Derijard, B., Hibi, M., Wu, I.H., Barret, T., Su, B., Deng, T., Karin, M., 1994. JNK: a protein kinase stimulated by UV light and Ha-Ras that binds and phosphorylates the c-Jun activation domain. Cell 76, 1025–1037.

Eberhardt, W., Huwiler, A., Beck, K.F., Walpen, S., Pfeilschifter, J., 2000. Amplification of IL-1beta-induced matrix metalloproteinase-9 expression by superoxide in rat glomerular mesangial cells is mediated by increased activities of NF-kappaB and activating protein-1 and involves activation of the mitogen-activated protein kinase pathways. Journal of Immunology 165, 5788–5797.

Benbow, U., Brinckerhoff, C.E., 1997. The AP-1 site and MMP gene regulation: what is all the fuss about?. Matrix Biolology 15, 519–526.

Chen, A., Davis, B.H., 1999. UV irradiation activates JNK and increases alphaI(I) collagen gene expression in rat hepatic stellate cells. Journal of Biological Chemistry 274, 158–164.

Cuenda, A., Rouse, J., Doza, Y.N., Meier, R., Cohen, P., Gallangher, T.F., Young, P.R., 1995. SB 203580 is a specific inhibitor of a MAP kinase homologue which is stimulated by cellular stresses and interleukin-1. FEBS Letter 364, 229–233.

Dudley, D.T., Pang, L., Decker, S.T., Bridges, A.J., Saltiel, A.R., 1995. A synthetic inhibitor of the mitogen-activated protein kinase cascade. Proceedings of the National Academy of Science U.S.A. 92, 7686–7689.

Durko, M., Navab, R., Shibata, H.R., Brodt, P., 1997. Suppression of basement membrane type IV collagen degradation and cell invasion in human melanoma cells expressing an antisense RNA for MMP-1. Biochimica et Biophysica Acta 1356, 271–280.

Esparza, J., Vilardell, C., Calvo, J., Juan, M., Vives, J., Urbano-Marquez, A., Yague, J., 1999. Fibronectin upregulates gelatinase B (MMP-9) and induces coordinated expression of gelatinase A (MMP-2) and its activator MT1-MMP (MMP-14) by human T lymphocyte cell lines. A process repressed through RAS/MAP kinase signaling pathways. Blood 94, 2754–2766.

Friedman, S.L., 1991. The cellular basis of hepatic fibrosis. Mechanisms and treatment strategies. New England Journal of Medicine 328, 1828–1835.

Han, J., Lee, J.D., Bibbs, L., Ulevitch, R.J., 1994. A MAP kinase targeted by endotoxin and hyperosmolarity in mammalian cells. Science 265, 808–811.

Herron, G.S., Banda, M.J., Clark, E.J., Gavrilovic, J., Werb, Z., 1986. Secretion of metalloproteinases by stimulated capillary endothelial cells. Journal of Biological Chemistry 261, 2814–2818.

Hironaka, K., Sakaida, I., Matsumura, Y., Kaino, S., Miyamoto, K., Okita, K., 2000. Enhanced interstitial collagenase (matrix metalloproteinase-13) production of Kupffer cells by gadolinium chrolide prevents pig serum-induced rat liver fibrosis. Biochemical and Biophysical Research Communications 267, 290–295.

Iredale, J.P., Benyon, R.C., Arthur, M.J., Ferris, W.F., Alcolado, R., Winwood, P.J., Clark, N., 1996. Tissue inhibitor of metalloproteinase-1 messenger RNA expression is enhanced relative to interstitial collagenase messenger RNA in experimental liver injury and fibrosis. Hepatology 24, 176–184.

Kayano, K., Sakaida, I., Uchida, K., Okita, K., 1998. Inhibitory effects of the herbal medicine Sho-saiko-to (TJ-9) on cell proliferation and procollagen gene expressions in cultured rat hepatic stellate cells. Journal of Hepatology 29, 642–649.

Kato, M., Liu, W., Yi, H., Asai, N., Hayakawa, A., Kozaki, K., Takahashi, M., Nakashima, I., 1998. The herbal medicine Sho-saiko-to inhibits growth and metastasis of malignant melanoma primarily developed in ret-transgenic mice. Journal of Investigative Dermatology 111, 640–644.

Kyriakis, J.M., Banerjee, P., Nikolakaki, E., Dai, T., Rubie, E.A., Ahmed, M.F., Avruch, J., 1994. The stress-activated protein kinase subfamily of c-Jun kinases. Nature 369, 156–160.

Lee, O.H., Bae, S.K., Bae, M.H., Lee, Y.M., Moon, E.J., Cha, H.J., Kwon, Y.G., 2000. Identification of angiogenic properties of insulin-like growth factor II in in vitro angiogenesis models. British Journal of Cancer 82, 385–391.

Li, W.Q., Zafarullah, M., 1998. Oncostatin M up-regulates tissue inhibitor of metalloproteinases-3 gene expression in articular chondrocytes via de novo transcription, protein synthesis, and tyrosine kinase- and mitogen-activated protein kinase-dependent mechanisms. Journal of Immunology 161, 5000–5007.

Matsuzaki, Y., Kurokawa, F., Terai, S., Matsumura, Y., Kobayashi, N., Okita, K., 1996. Cell death induced by baicalein in human hepatocellular carcinoma cell lines. Japanese Journal of Cancer Research 87, 170–177.

Merchant, J.L., Du, M., Todisco, A., 1999. Sp1 phosphorylation by Erk 2 stimulates DNA binding. Biochemical and Biophysical Research Communications 254, 454–461.

Oka, H., Yamamoto, S., Kanno, T., Kuroki, T., Mizoguchi, Y., Kobayashi, K., 1995. Controlled prospective evaluation of Sho-saiko-to in prevention of hepatocellular carcinoma in patients with cirrhosis of the liver. Cancer 76, 743–749.

Okita, K., Li, Q., Murakami, T., Takahashi, M., 1993. Anti-growth effects with components of Sho-saiko-to (TJ-9) on cultured human hepatoma cells. European Journal of Cancer Prevention 2, 169–176.

Okita, K., Kurokawa, F., Yamasaki, T., Furukawa, T., Li, Q., Murakami, T., 1994. The use of Sho-saiko-to (TJ-9) for chemoprevention of chemical hepatocarcinogenesis in rats and discussion of its possible pharmacologic action. Transgenica 1, 39–44.

Ravanti, L., Hakkinen, L., Larjava, H., Saarialho-Kere, U., Foschi, M., Han, J., Kahari, V.M., 1999a. Transforming growth factor-beta induces collagenase-3 expression by human gingival fibroblasts via p38 mitogen-activated protein kinase. Journal of Biological Chemistry 274, 37292–37300.

Ravanti, L., Heino, J., Lopez-Otin, C., Kahari, V.M., 1999b. Induction of collagenase-3 (MMP-13) expression in human skin fibroblasts by three-dimensional collagen is mediated by p38 mitogen-activated protein kinase. Journal of Biological Chemistry 274, 2446–2455.

Sato, H., Takino, T., Okada, Y., Cao, J., Shinagawa, A., Yamamoto, E., Seiki, M., 1994. A matrix metalloproteianse expressed on the surface of invasive tumour cells. Nature 370, 61–65.

Sakaida, I., Matsumura, Y., Kubota, M., Kayano, K., Takenaka, K., Okita, K., 1996. The prolyl 4-hydroxylase inhibitor HOE 077 prevents activation of Ito cells, reducing procollagen gene expression in rat liver fibrosis induced by choline deficient L-amino acid-defined diet. Hepatology 23, 755–763.

Sakaida, I., Matsumura, Y., Akiyama, S., Hayashi, K., Ishige, A., Okita, K., 1998a. Herbal medicine Sho-saiko-to (TJ-9) prevents liver fibrosis and enzyme-altered lesions in rat liver cirrhosis induced by a choline-deficient L-amino acid-defined diet. Journal of Hepatology 28, 298–306.

Sakaida, I., Hironaka, K., Uchida, K., Kayano, K., Okita, K., 1998b. Fibrosis accelerates the development of enzyme-altered lesions in the rat liver. Hepatology 28, 1247–1252.

Sakaida, I., Uchida, K., Hironaka, K., Okita, K., 1999. Prolyl 4-hydroxylase inhibitor (HOE 077) prevents TIMP-1 gene expression in rat liver fibrosis. Journal of Gastroenterology 34, 376–377.

Shimizu, I., Ma, Y.R., Mizobuchi, Y., Liu, F., Miura, T., Nakai, Y., Yasuda, M., Amagaya, S., Kawada, N., Hori, H., Ito, S., 1999. Effects of Sho-saiko-to, a Japanese herbal medicine, on hepatic fibrosis in rats. Hepatology 29, 149–160.

Simon, C., Goepfert, H., Boyd, D., 1998. Inhibition of the p38 mitogen-activated protein kinase by SB 203580 blocks PMA-induced Mr 92,000 type IV collagenase secretion and in vitro invasion. Cancer Research 58, 1135–1139.

Solis-Herruzo, J.A., Rippe, R.A., Schrum, L.W., de La Torre, P., Garcia, I., Jeffrey, J.J., Munoz-Yague, T., 1999. Interleukin-6 increases rat metalloproteinase-13 gene expression through stimulation of activator protein 1 transcription factor in cultured fibroblasts. Journal of Biological Chemistry 274, 30919–30926.

Tatsuta, M., Ishii, H., Baba, M., Nakaizumi, A., Uehara, H., 1991. Inhibition by xiao-chai-hu-tang (TJ-9) of development of hepatic foci induced by N-nitrosomorpholine in Sprague-Dawley rats. Japanese Journal of Cancer Research 82, 987–992.

Trim, J.E., Samra, S.K., Arthur, M.J., Wright, M.C., McAulay, M., Beri, R., Mann, D.A., 2000. Upstream tissue inhibitor of metalloproteinases-1 (TIMP-1) element-1, a novel and essential regulatory DNA motif in the human TIMP-1 gene promoter, directly interacts with a 30-kDa nuclear protein. Journal of Biological Chemistry 275, 6657–6663.

Underwood, D.C., Osborn, R.R., Bochnowicz, S., Webb, E.F., Rieman, D.J., Lee, J.C., Romanic, A.M., 2000. SB 239063, a p38 MAPK inhibitor, reduces neutrophilia, inflammatory cytokines, MMP-9, and fibrosis in lung. American Journal of Physiology-Lung Cellular and Molecular Physiology 279, L895–L902.

Wang, M., Hu, Y., Shima, I., Stearns, M.E., 1998. Identification of positive and negative regulator elements for the tissue inhibitor of metalloproteinase 1 gene. Oncology Research 10, 219–233.

Yamamoto, K., Araki, N., Ogawa, K., 1985. Ultrastructural and ultracytochemical examination of the effects of preadministration of Xia-Chai-Hu-Tang on hepatic disorders induced by D-galactosamine Hcl. Acta Histochemia et Cytochemica 18, 403–418.

Yano, H., Mizoguchi, A., Fukuda, K., Haramaki, M., Ogasawara, S., Momosaki, S., Kojiro, M., 1994. The herbal medicine Sho-saiko-to inhibits proliferation of cancer cell lines by inducing apoptosis and arrest at the G0/G1 phase. Cancer Research 54, 448–454.

Zeigler, M.E., Chi, Y., Schmidt, T., Varani, J., 1999. Role of ERK and JNK pathways in regulating cell motility and matrix metalloproteinase 9 production in growth factor-stimulated human epidermal keratinocytes. Journal of Cellular Physiology 180, 271–284.

Proteomics 2004, *4*, 2111–2116 DOI 10.1002/pmic.200300712

Proteomic profiling of proteins decreased in hepatocellular carcinoma from patients infected with hepatitis C virus

Yuichiro Yokoyama[1, 2], Yasuhiro Kuramitsu[2], Motonari Takashima[3], Norio Iizuka[4], Toshifusa Toda[5], Shuji Terai[1], Isao Sakaida[1], Masaaki Oka[3], Kazuyuki Nakamura[2] and Kiwamu Okita[1]

[1]Department of Gastroenterology and Hepatology
[2]Department of Biochemistory and Biomolecular Recognition
[3]Department of Surgery II
[4]Department of Bioregulatory Function,
Yamaguchi University School of Medicine, Yamaguchi, Japan
[5]Tokyo Metropolitan Institute of Gerontology, Tokyo, Japan

Hepatocellular carcinoma (HCC) is a major cause of death in Japan. It has been suggested that hepatitis C virus (HCV) plays an important role in hepatocarcinogenesis, because of high incidence among the patients. To understand the mechanism of hepatocarcinogenesis after HCV infection, we performed a comparative study on the protein profiles between tumorous and nontumorous specimens from the patients infected with HCV by means of two-dimensional electrophoresis. Eleven spots were decreased in HCC tissues from over 50% of the patients. Eight proteins out of 11 spots were identified using peptide mass fingerprinting with matrix-assisted laser desorption/ionization-time of flight-mass spectrometry. These proteins were liver type aldolase, tropomyosin β-chain, ketohexokinase, enoyl-CoA hydratase, albumin, smoothelin, ferritin light chain, and arginase 1. The intensity of enoyl-CoA hydratase, tropomyosin β-chain, ketohexokinase, liver type aldolase, and arginase 1 was significantly different ($p < 0.05$). The decrease of 8 proteins was characteristic in HCC. We will discuss the implication of these proteins for the loss of function of hepatocytes and for the possibility of carcinogenesis of HCV-related HCC.

Received	24/9/03
Revised	25/11/03
Accepted	09/12/03

Keywords: Hepatitis C virus / Hepatocellular carcinoma / Liver proteome / Two-dimensional gel electrophoresis

1 Introduction

Hepatocellular carcinoma (HCC) can be caused by chronic infection of hepatitis B or C virus. Particularly, in Japan most patients of HCC are hepatitis C virus (HCV)-positive. Accordingly, HCV may play an important role in hepatocarcinogenesis. That is, HCV carriers proceed to chronic hepatitis, to liver cirrhosis, and to HCC after incubation periods of 15, 25, and 30 years in average, respectively [1, 2]. HCC-specific markers, if present, are reliable for its early detection and for better understanding hepatocarcinogenesis. From this aspect, search for HCC-specific transcripts has been performed by means of cDNA microarray [3–10]. Iizuka *et al.* [5] reported that many genes for detoxification and immune response were upregulated in HCV-related HCC. However, expression of genes and proteins are not always uniform. Therefore, recently many studies of proteome were reported for understanding of mechanism of diseases by two-dimensional gel electrophoresis (2-DE). HCC was no exception [11–14]. Tannapfel *et al.* [15] showed that 5 proteins (insulin growth factor II, a disintegrin and metalloproteases, signal transducers and activators of transcription 3, suppressors of cytokine signaling 3, and cyclin D1) was significantly upregulated and 4 proteins (collagen i, SMAD 4, fragile histidine triad, and suppressors of cytokine signaling 1) were downregulated in HCC by protein

Correspondence: Prof. Kazuyuki Nakamura, Department of Biochemistory and Biomolecular recognition, Yamaguchi University School of Medicine, 1-1-1 Minamikogushi, Ube, Yamaguchi, 755-8505, Japan
E-mail: nakamura@yamaguchi-u.ac.jp
Fax: +81-836-22-2212

Abbreviations: HBs-Ag, hepatitis B surface antigen; **HBV**, hepatitis B virus; **HCC**, hepatocellular carcinoma; **HCV**, hepatitis C virus; **HCV-Ab**, anti-hepatitis C virus antibody

microarrays. We tried to analyze proteomics using HCV-positive HCC specimens in comparison with the surroundings. We already reported the expression of heat shock protein 70 family members increased in HCV-related HCC tissues [16].

2 Materials and methods

2.1 Tissue specimens

We examined tumorous and paired nontumorous liver specimens from 20 patients who had undergone partial hepatectomy for HCC at the Yamaguchi University Hospital between 1998 and 2000. All were positive for anti-HCV antibody (HCV-Ab) and negative for hepatitis B surface antigen (HBs-Ag). Four patient 's HCCs were well differentiated, 15 were moderately differentiated, and the last one was poorly differentiated. Twelve out of the 20 nontumorous tissues indicated cirrhotic liver.

2.2 Sample preparation

Resected liver tissues which were immediately frozen in liquid nitrogen and stored at −80°C were disrupted in lysis buffer (1% NP-40, 1 mM sodium vanadate, 1 mM PMSF, 50 mM Tris, 10 mM NaF, 10 mM EDTA, 165 mM NaCl, 10 μg/mL leupeptin, 10 μg/mL aprotinin) using a Potter type homogenizer with a Teflon tip at 4°C for 1 h. The lysate was separated by centrifugation at 15 000 × *g* for 30 min to yield supernatant that was stored at −80°C.

2.3 Two-dimensional gel electrophoresis (2-DE)

The supernatant from liver tissues (300 μg) was applied to Immobiline dry strips (pH 3–10, 7 cm; Amersham Pharmacia Biotechnology, Uppsala, Sweden) in a total volume of 125 μL containing 8 M urea, 2% CHAPS and 0.5% IPG buffer (Amersham Pharmacia Biotechnology) and 2.8 mg/mL dithiothreitol (DTT). After rehydration for 14 h, proteins were separated by isoelectrofocusing (IEF) at 20°C and 50 μA/strip with the following linear voltage increases: 500 V for 1 h, 1000 V for 1 h, and 8000 V for 2 h. The strips were then equilibrated twice in 50 mM Tris containing 6 M urea, 30% glycerol and 2% sodium dodecyl sulfate (SDS) for 10 min. Dithiothreitol was then added, followed by iodoacetamide. The second dimension proceeded on 12.5% nongradient SDS-polyacrylamide gels (24.5 cm × 11 cm: SDS-PAGE) at two steps: 600 V, 20 mA for 30 min and 600 V, 50 mA for 70 min in a Multiphor horizontal electrophoresis unit (Amersham Pharmacia Biotechnology). Separated protein spots were fixed and stained on the gel with 30% methanol, 10% acetic acid, and 0.1% Coomassie Brilliant Blue R-250 (CBB) overnight. The gel was destained with 30% methanol and 10% acetic acid for 30 min, and then with 7% acetic acid until the stain of background was clear and colorless.

2.4 Image analysis

The positions of the protein spots on tumorous and nontumorous tissues were recorded using an Agfa ARCUS 1200™ image scanner (Agfa-Gevaert N.V., Mortsel, Belgium) and analyzed with PDQUEST computer software Ver. 7.1 (Bio-Rad Laboratories, Hercules, CA, USA). Spots stained at different intensities were excised from the gels and identified by peptide mass fingerprinting with matrix-assisted laser desorption/ionization-time of flight-mass spectrometry (MALDI-TOF-MS).

2.5 In-gel digestion

The CBB dye was removed by rinsing twice in 60% methanol containing 50 mM ammonium bicarbonate and 5 mM DTT for each 15 min, and twice in 50% acetonitrile containing 50 mM ammonium bicarbonate and 5 mM DTT for each 7 min. The gel piece was dehydrated in 100% acetonitrile, and then reswollen with an in-gel digestion reagent containing 10 μg/mL sequencing-grade trypsin (Promega, Madison, WI, USA) in 30% acetonitrile of 50 mM ammonium bicarbonate and 5 mM DTT. The in-gel digestion was performed overnight at 30°C.

2.6 Peptide mass fingerprinting

After in-gel digestion, 1 μL of the reaction mixture was removed and mixed with 1 μL of matrix solution (10 mg/mL α-cyano-4-hydroxycinnamic acid in 50% acetonitrile, 40% methanol, 0.1% trifluoroacetic acid) on a MALDI target plate. MALDI-TOF-MS for peptide mass fingerprinting was performed on AXIMA-CFR mass spectrometer (Shimadzu Biotech, Kyoto, Japan) in reflectron mode. The MS-Fit database search engine in the Protein Prospector web site (http://prospector.ucsf.edu/) was used for protein identification.

2.7 Immunoblot analysis

Samples of 7 μg were separated by SDS-PAGE at 15 mA. After SDS-PAGE, the fractionated proteins were transferred electrophoretically to a PVDF membrane (Immobilon; Millipore, Bedford, MA, USA) and blocked overnight at 4°C with TBS containing 5% skim milk. Primary antibodies used were anti-aldolase B polyclonal antibody (1:100) and anti-arginase 1 polyclonal antibody (1:100)

(all from Santa Cruz Biotechnology, Santa Cruz, CA, USA). For each, membranes were incubated for 1 h, washed four times with TBS containing 0.05% Tween 20, incubated for 1 h with horseradish peroxidase-conjugated secondary antibody (1:2000) (ICN Pharmaceuticals, Aurora, OH, USA), and developed with a chemiluminescence reagent (ECL; Amersham Pharmacia Biotechnology).

3 Results

We compared the differential expression of proteins by 2-DE of paired tumorous and nontumorous liver tissues from 20 patients with HCC. Staining with CBB R-250 detected about 480 protein spots (Fig. 1). Eleven of these were decreased in tumorous tissues from over 50% of the patients. Peptide mass fingerprinting with MALDI-TOF-MS identified ketohexokinase, arginase 1, liver type aldolase, enoyl-CoA hydrase, tropomyosin β-chain, albumin, smoothelin, and ferritin light chain (Fig. 2). Information about the 11 spots and the 8 identified proteins are summarized in Table 1. The expression of arginase 1 was decreased in 95% of HCC patients. Liver-type aldolase was decreased in 85%, tropomyosin β-chain in 80%, ketohexokinase, enoyl-CoA hydrase and albumin in 70%, smoothelin in 65%, and ferritin light chain in tumorous tissues from 60% patients. We performed pairwise *t*-tests between the means of spot intensity of tumorous tissues and nontumorous tissues. The intensity of enoyl-CoA hydratase, toropomyosin β-chain, ketohexokinase, liver type aldolase, and arginase 1 significantly differed between tumorous and nontumorous tissues (Fig. 3). The

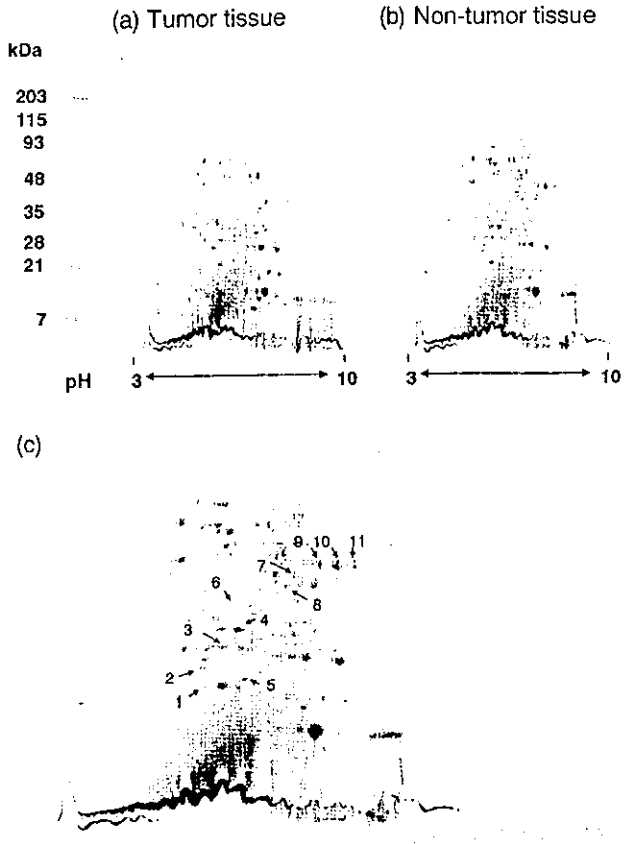

Figure 1. Two-dimensional gel electrophoresis map of human liver tissue. (a) Tumorous tissue, (b) nontumorous tissue of a HCC patient infected with HCV. Proteins (300 μg) were separated on 12.5% nongradient polyacrylamide gels and stained with CBB. (c) Enlarged 2-DE map from (b); protein spots are numbered from 1 to 11.

Table 1. Protein spots that decreased in HCC tissues

Spot No.[a]	Accession No.	Protein	Number of patients[b] (%)	Spot intensity (average ± SD)		Ratio of spot intensity[c] (% average ± SD)
				Tumorous tissue	Nontumorous tissue	
1	P53814	Smoothelin	13 (65%)	2 466.2 ± 3 333.6	2 872.8 ± 1 688.4	108.57 ± 115.09
2	P02792	Ferritin light chain	12 (60%)	2 601.1 ± 2 590.2	2 936.4 ± 2 408.1	286.52 ± 521.40
3	P02768	Albumin	14 (70%)	25 635.1 ± 77 312.6	12 585.5 ± 11 585.3	189.58 ± 401.46
4	P30084	Enoyl-CoA hydratase	14 (70%)	13 110.9 ± 15 939.1	27 113.4 ± 19 645.5	86.66 ± 112.12
5	P07951	Tropomyosin β-chain	16 (80%)	1 780.7 ± 1 423.4	4 984.9 ± 5 349.2	59.20 ± 50.69
6	P50053	Ketohexokinase	14 (70%)	1 842.2 ± 1 534.1	3 407.6 ± 1 951.5	107.36 ± 181.62
7	P05089	Arginase 1	19 (95%)	2 394.0 ± 2 331.7	7 460.4 ± 5 742.2	99.36 ± 299.39
8	P05062	Liver-type aldolase	17 (85%)	2 321.1 ± 1 766.5	5 822.9 ± 6 591.3	104.30 ± 195.60
9	P05062	Liver-type aldolase	17 (85%)	4 705.5 ± 5 199.0	20 619.2 ± 26 706.9	48.73 ± 67.16
10	P05062	Liver-type aldolase	18 (90%)	6 122.1 ± 3 997.5	60 282.2 ± 161 480.1	57.40 ± 107.92
11	P05062	Liver-type aldolase	17 (85%)	22 109.5 ± 19 933.8	113 699.8 ± 164 866.2	61.97 ± 105.57

a) Spot numbers correspond to that in Fig. 1c.
b) Number of patients in which protein expression decreased in tumorous tissues
c) Percentage of spot intensity of tumorous to nontumorous tissues calculated for each sample pair

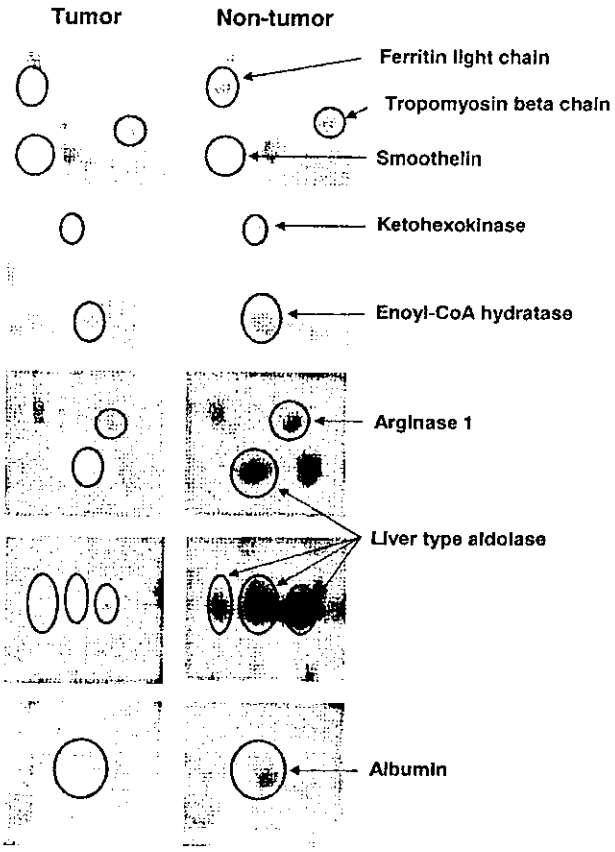

Figure 2. Downregulated expression of 11 spots and 8 proteins in HCC. Spots of all 11 proteins that decreased in tumorous tissues include smoothelin, ferritin light chain, tropomyosin β-chain, albumin, ketohexokinase, enoyl-CoA hydratase, liver type aldolase, and arginase 1.

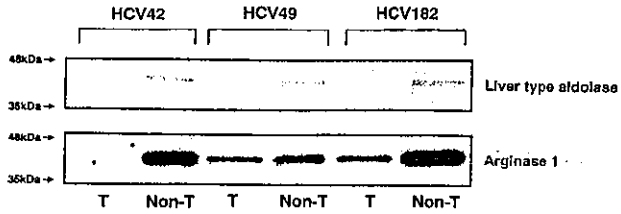

Figure 4. Immunoblot analysis of liver-type aldolase (aldolase B) and arginase 1. Expression of the two proteins was confirmed and the intensity of each band was less in tumorous tissues (T) than in nontumorous tissues (Non-T). Three samples (HCV42, HCV49, and HCV182) from 20 were shown. The molecular weight markers are indicated by arrows.

expression of two proteins among five, liver type aldolase and arginase 1, whose antibodies were available, was confirmed by immunoblot analysis. The intensity of each band was less in tumorous tissues than in nontumorous tissues (Fig. 4).

4 Discussion

There were some previous proteomic studies for HCC, and the etiologies of their HCCs were abundant. Many of them were hepatitis B virus (HBV)-related HCCs [11–14]. However, all of the patients of our study were HCV-Ab-positive and HBs-Ag-negative. Since the hepatocarcinogenetic mechanism of HCV may be different from HBV, we need to construct several databases of HBV- and HCV-related HCCs. We found that the decrease of keto-

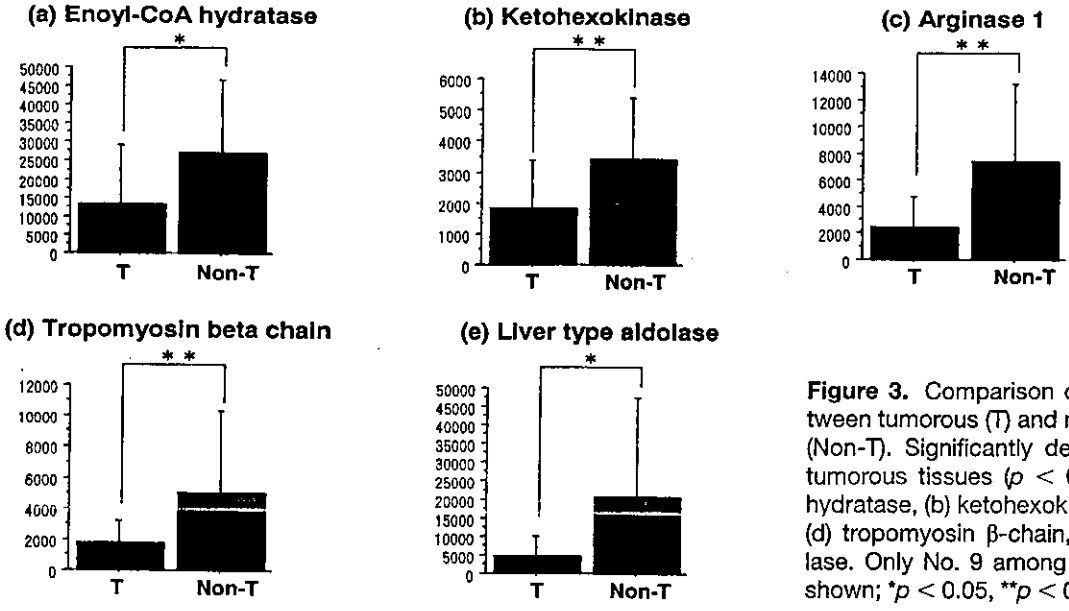

Figure 3. Comparison of spot intensity between tumorous (T) and nontumorous tissues (Non-T). Significantly decreased proteins in tumorous tissues ($p < 0.05$): (a) enoyl-CoA hydratase, (b) ketohexokinase, (c) arginase 1, (d) tropomyosin β-chain, (e) liver type aldolase. Only No. 9 among 4 aldolase spots is shown; $^{*}p < 0.05$, $^{**}p < 0.01$.

hexokinase, ferritin light chain, and enzymes involved in the glycolysis and mitochondrial β-oxidation pathways concurs with other human HCC proteomic studies. We discovered also the decrease of smoothelin and tropomyosin β-chain. The proteins which we detected in this study are classified as metabolic enzymes and cytoskeletal proteins. Smoothelin and tropomyosin β-chain belong to the latter. Smoothelin is a cytoskeletal protein existing in visceral and vascular smooth muscle cells [17] as 59 kDa smoothelin-A and 110 kDa smoothelin-B [18, 19]. Rensen *et al.* [20] could not detect smoothelin in normal liver by Western blotting. However, we could detect by 2-DE smoothelin on both gels of tumorous and nontumorous tissues from patients infected with HCV. The use of samples infected with HCV may cause this discrepancy. Hepatic stellate cells (HSCs) have fatty droplets including vitamin A and regulate the sinusoidal microcirculation in normal liver [21, 22]. Once liver tissues are injured, HSCs are activated and change their structure and function. Activated HSCs transform themselves into the myofibroblast and lead to overexpression of α-smooth muscle actin [23, 24]. These data indicated that the source of smoothelin might be not hepatocytes but intermediate cells. Although smoothelin may not be specific to cancer cells, interaction between cancer cells and intermediate cells is important. In accordance with progression of hepatocarcinogenesis, cancer tissues destroy hepatic cords. Therefore, smoothelin may become a marker of HCC progression.

Tropomyosin binds to actin filaments in muscle as well as nonmuscle cells, and regulates muscle contraction in conjunction with troponin. Tropomyosin is a heterodimer of α- and β-chains. In nonmuscle cells such as hepatocytes, tropomyosin plays a role of stabilization of actin filaments [25, 26]. It was reported that tropomyosin suppressed the transformation of phenotypes in nonmuscle cells [27–29]. In previous proteomic studies using 2-DE, the expression of tropomyosin-2 decreased in human ovarian cancer tissues [30] and the expression of tropomyosin β-chain decreased in human prostate cancer tissues [31]. In addition, the expression of tropomyosin decreased in several cancer tissues [30–33].

In metabolic enzymes, the expression of liver-type aldolase considerably decreased in our tumorous tissues, and this decrease has never been reported in previous proteomic studies on human HCCs. Aldolase performs the sixth step of glycolysis. Aldolase has three isozymes. Aldolase A exists in muscle, aldolase B in liver, and aldolase C in brain [34]. Weinhouse *et al.* [35] have shown that liver-type aldolase was replaced by nonliver type aldolase in poorly differentiated rat liver tumors. Kinoshita *et al.* [36] have reported that the mRNA of aldolase B was downexpressed in 18 of 20 HCC patients, and Kimura *et al.* [37] found that the expression level of aldolase B was low and aldolase A was high in hepatoma cell lines. Salvatore *et al.* [38] have shown that the mRNA expression of aldolase A in HCC tissues was higher than that in surrounding cirrhotic tissues. Aldolase A is exclusively expressed in the fetal liver [39]. As the expression of carcinoembryonic antigen (CEA) or α-fetoprotein (AFP) which are expressed during embryonic or fetal terms increase in cancer tissues, the expression of aldolase A might increase in HCC tissues by replacing aldolase B. We found the spots of albumin and smoothelin at different positions from those predicted by the p*I* value and molecular weight on both gels of tumorous and nontumorous tissues. These results might be caused by post-translational modifications or mutation by HCV infection. These changes could be characteristic of HCV-related HCCs.

In this study, we performed the first proteomic analysis of human HCV-related HCCs. A protein expression database constructed by reference to our study may be useful for the discovery of new tumor markers and for producing new diagnostic techniques.

This study was supported a Grant-in-Aid for Scientific Reserch from the Japan Society for the Promotion of Science (No. 13470121 to Shuji Terai, Isao Sakaida, and Kiwamu Okita; No. 13770262 to Shuji Terai) and a Grant-in-Aid for translational research from the Ministry of Health, Labor and Welfare (H-trans-5 to Shuji Terai, Isao Sakaida, Hiroshi Nishina and Kiwamu Okita).

5 References

[1] Tanaka, E., Kiyosawa, K., *J. Gastroenterol. Hepatol.* 2000, *15*, E97–E104.

[2] Niederau, C., Lange, S., Heintges, T., Erhardt, A., *et al.*, *Hepatology* 1998, *28*, 1687–1695.

[3] Smith, M. W., Yue, Z. N., Geiss, G. K., Sadovnikova, N. Y., *et al.*, *Cancer Res.* 2003, *63*, 859–864.

[4] Chung, E. J., Sung, Y. K., Farooq, M., Kim, Y., *et al.*, *Mol. Cells* 2002, *14*, 382–387.

[5] Iizuka, N., Oka, M., Yamada-Okabe, H., Mori, N., *et al.*, *Cancer Res.* 2002, *62*, 3939–3944.

[6] Xu, X. R., Huang, J., Xu, Z. G., Qian, B. Z., *et al.*, *Proc. Natl. Acad. Sci. USA* 2001, *98*, 15089–15094.

[7] Takeo, S., Arai, H., Kusano, N., Harada, T., *et al.*, *Cancer Genet. Cytogenet.* 2001, *130*, 127–132.

[8] Shirota, Y., Kaneko, S., Honda, M., Kawai, H. F., Kobayashi, K., *Hepatology* 2001, *33*, 832–840.

[9] Okabe, H., Satoh, S., Kato, T., Kitahara, O., *et al.*, *Cancer Res.* 2001, *61*, 2129–2137.

[10] Lau, W. Y., Lai, P. B., Leung, M. F., Leung, B. C., *et al.*, *Oncol. Res.* 2000, *12*, 59–69.

[11] Park, K. S., Cho, S. Y., Kim, H., Paik, Y. K., *Int. J. Cancer* 2002, *97*, 261–265.

[12] Park, K. S., Kim, H., Kim, N. G., Cho, S. Y., *et al.*, *Hepatology* 2002, *35*, 1459–1466.

[13] Kim, J., Kim, S. H., Lee, S. U., Ha, G. H., *et al.*, *Electrophoresis* 2002, *23*, 4142–4156.

[14] Lim, S. O., Park, S. J., Kim, W., Park, S. G., *et al.*, *Biochem. Biophys. Res. Commun.* 2002, *291*, 1031–1037.

[15] Tannapfel, A., Anhalt, K., Hausermann, P., Sommerer, F., *et al.*, *J. Pathol.* 2003, *201*, 238–249.

[16] Takashima, M., Kuramitsu, Y., Yokoyama, Y., Iizuka, T., *et al.*, *Proteomics* 2003, *3*, 2487–2493.

[17] van der Loop, F. T., Schaart, G., Timmer, E. D., Ramaekers, F. C., van Eys, G. J., *J. Cell Biol.* 1996, *134*, 401–411.

[18] van Eys, G. J., Voller, M. C., Timmer, E. D., Wehrens, X. H., *et al.*, *Cell Struct. Funct.* 1997, *22*, 65–72.

[19] Wehrens, X. H., Mies, B., Gimona, M., Ramaekers, F. C., *et al.*, *FEBS. Lett.* 1997, *405*, 315–320.

[20] Rensen, S. S., Thijssen, V. L., De Vries, C. J., Doevendans, P. A., *et al.*, *Cardiovasc. Res.* 2002, *55*, 850–863.

[21] Blomhoff, R., Rasmussen, M., Nilsson, A., Norum, K. R., *et al.*, *J. Biol. Chem.* 1985, *260*, 13560–13565.

[22] Wake, K., *Int. Rev. Cytol.* 1980, *66*, 303–353.

[23] Schurch, W., Seemayer, T. A., Gabbiani, G., *Am. J. Surg. Pathol.* 1998, *22*, 141–147.

[24] Ramadori, G., Veit, T., Schwogler, S., Dienes, H. P., *et. al.*, *Virchows Arch. B* 1990, *59*, 349–357.

[25] Ishikawa, R., Yamashiro, S., Matsumura, F., *J. Biol. Chem.* 1989, *264*, 16764–16770.

[26] Ishikawa, R., Yamashiro, S., Matsumura, F., *J. Biol. Chem.* 1989, *264*, 7490–7497.

[27] Bhattacharya, B., Prasad, G. L., Valverius, E. M., Salomon, D. S., Cooper, H. L., *Cancer Res.* 1990, *50*, 2105–2112.

[28] Mahadev, K., Raval, G., Bharadwaj, S., Willingham, M. C., *et al.*, *Exp. Cell Res.* 2002, *279*, 40–51.

[29] Bharadwaj, S., Prasad, G. L., *Cancer Lett.* 2002, *183*,205–213.

[30] Alaiya, A. A., Franzen, B., Fujioka, K., Moberger, B., *et al.*, *Int. J. Cancer* 1997, *73*, 678–683.

[31] Ahram, M., Best, C. J., Flaig, M. J., Gillespie, J. W., *et al.*, *Mol. Carcinog.* 2002, *33*, 9–15.

[32] Jung, M. H., Kim, S. C., Jeon, G. A., Kim, S. H., *et al.*, *Genomics* 2000, *69*, 281–286.

[33] Tada, A., Kato, H., Hasegawa, S., *Oncol. Rep.* 2000, *7*, 1323–1326.

[34] Taguchi, K., Takagi, Y., *Rinsho Byori* 2001, *Suppl. 116*, 117–124.

[35] Adelman, R. C., Morris, H. P., Weinhouse, S., *Cancer Res.* 1967, *27*, 2408–2413.

[36] Kinoshita, M., Miyata, M., *Hepatology* 2002, *36*, 433–438.

[37] Kimura, T., *Hokkaido Igaku Zasshi* 1994, *69*, 1232–1243.

[38] Castaldo, G., Calcagno, G., Sibillo, R., Cuomo, R., *et al.*, *Clin. Chem.* 2000, *46*, 901–906.

[39] Costanzo, P., Izzo, P., Lupo, A., Rippa, E., *et al.*, *Ital. J. Biochem.* 1988, *37*, 8–13.

Transplantation of Bone Marrow Cells Reduces CCl_4-Induced Liver Fibrosis in Mice

Isao Sakaida,[1] Shuji Terai,[1] Naoki Yamamoto,[1] Koji Aoyama,[1] Tsuyoshi Ishikawa,[1] Hiroshi Nishina,[2] and Kiwamu Okita[1]

We investigated the effect of bone marrow cell (BMC) transplantation on established liver fibrosis. BMCs of green fluorescent protein (GFP) mice were transplanted into 4-week carbon tetrachloride (CCl_4)–treated C57BL6 mice through the tail vein, and the mice were treated for 4 more weeks with CCl_4 (total, 8 weeks). Sirius red and GFP staining clearly indicated migrated BMCs existing along with fibers, with strong expression of matrix metalloproteinase (MMP)-9 shown by anti–MMP-9 antibodies and *in situ* hybridization. Double fluorescent immunohistochemistry showed the expression of MMP-9 on the GFP-positive cell surface. Film *in situ* zymographic analysis revealed strong gelatinolytic activity in the periportal area coinciding with the location of MMP-9–positive BMCs. Four weeks after BMC transplantation, mice had significantly reduced liver fibrosis, as assessed by hydroxyproline content of the livers, compared to that of mice treated with CCl_4 alone. Subpopulation of Liv8-negative BMCs was responsible for this fibrolytic effect. In conclusion, mice with BMC transplants with continuous CCl_4 injection had reduced liver fibrosis and a significantly improved survival rate after BMC transplantation compared with mice treated with CCl_4 alone. This finding introduces a new concept for the therapy of liver fibrosis. *Supplementary material for this article can be found on the HEPATOLOGY website (http://interscience.wiley.com/jpages/0270-9139/suppmat/index.html).* (HEPATOLOGY 2004;40: 1304–1311.)

Recent reports have shown the capacity of the bone marrow cell (BMC) to differentiate into a variety of non-hematopoietic cell lineages.[1–5] These results indicate that the BMC is an attractive cell source for regenerative medicine compared with tissue-specific stem cells.[6] The capacity of the BMC to differentiate into hepatocytes and intestinal cells has been shown by Y-chromosome detection in autopsy analysis of human female recipients of BMCs from male donors.[7,8] Although Lagasse et al. reported that purified hematopoietic stem cells could differentiate into hepatocytes using a fumarylacetate hydrase-deficient model,[5] Wagers et al. showed little evidence of plasticity in adult hematopoietic stem cells.[9] Thus, although there is still controversy about which part of BMCs can differentiate into hepatocytes, the BMC seems to have the plasticity to differentiate into such cells. From the point of view of therapy, one of the targets of liver disease for BMC transplantation is liver cirrhosis with chronic liver failure. This is an unphysiological condition with excessive deposition of extracellular matrix and a relative lack of parenchymal cells (hepatocytes). Even if BMC transplantation is successful in supplying parenchymal cells, the fate of the extracellular matrix under these conditions is unknown. The present study clearly shows that transplanted BMCs reduce (degrade) carbon tetrachloride (CCl_4)-induced liver fibrosis with a significantly improved survival rate.

Materials and Methods

Mice. GFP-transgenic mice (TgN(β-act-EGFP)Osb) were kindly provided by Masaru Okabe (Genome Research Center, Osaka University, Osaka, Japan).[10] C57BL6 female mice were purchased from Japan SLC

Abbreviations: BMC, bone marrow cell; CCl4, carbon tetrachloride; GFP, green fluorescent protein; PBS, phosphate-buffered saline; IgG, immunoglobulin G; MMP, matrix metalloproteinase; NGS, normal goat serum; NRS, normal rabbit serum; DIG, digoxigenin.

From the [1]Department of Gastroenterology and Hepatology, School of Medicine, Yamaguchi University, Yamaguchi, Japan; and [2]Department of Physiological Chemistry, Graduate School of Pharmaceutical Science, University of Tokyo, Tokyo, Japan.

Received September 30, 2003; accepted August 16, 2004.

Supported in part by grants-in-aid 16590597, 12670490, and 10470136 from the Ministry of Education, Culture, Sports, Science and Technology and by grants-in-aid for translational research from the Ministry of Health, Labor and Welfare of Japan.

Address reprint requests to: Isao Sakaida, M.D., Department of Gastroenterology and Hepatology, School of Medicine, Yamaguchi University, Minami-Kogushi 1-1-1 Ube, Yamaguchi-pref. 755-8505, Japan. E-mail: sakaida@yamaguchi-u.ac.jp; fax: (81) 836-22-2240.

Published online in Wiley InterScience (www.interscience.wiley.com).

DOI 10.1002/hep.20452

(Shizuoka, Japan). Mice were properly anesthetized during experiments.

Experimental Protocol. Six-week-old female C57BL6 mice were treated with 1 mL/kg CCl_4 dissolved in olive oil (1:1) twice a week for 4 weeks. One day (24 hours) after the eighth injection of CCl_4, 1×10^5 green fluorescent protein (GFP)-positive BMCs or sorted Liv8-positive or Liv8-negative BMCs (1×10^5 cells) or same volume of saline as a control (described also as mice treated with CCl_4 alone) were injected into the tail vein as described previously.[11,12] Mice continued to be treated with CCl_4. After 1, 2, 3, or 4 weeks, mice were then sacrificed to assess the extent of liver fibrosis. For examination of the survival rate, mice were treated with CCl_4 for 4 weeks and divided into 2 groups (15 mice each) with bone marrow transplantation or the same volume of saline injection. All mice were then treated with CCl_4 for a further 25 weeks.

BMC Preparation. For BMC isolation, GFP-transgenic mice (TgN(β-act-EGFP)Osb) (6 weeks old) were killed by cervical dislocation and the limbs removed. GFP-positive BMCs were flushed with Dulbecco's Modified Eagle medium (DMEM) culture medium with 10% fetal bovine serum (FBS) from the medullary cavities of tibias and femurs using a 25-G needle.

Production of Rat Monoclonal Antibody, Liv8. Eight-week old WKY/NCrj female rats were immunized in the hind footpads with 100 μg of E11.5 murine fetal liver lysate in complete Freund's adjuvant (0.2 mL). Anti-Liv8 antibodies were raised according to a previously described protocol.[13]

Fluorescence-Activated Cell Sorter Analysis of Fetal Liver Cells and BMCs Using Anti-Liv8 Antibody. Prepared mouse fetal liver cells (E11.5) and adult BMCs were reacted with biotin-conjugated anti-Liv8 antibody,[12] phycoerythrin-conjugated rat anti-CD45 (Becton Dickinson Bioscience, San Jose, CA), fluorescein isothiocyanate-conjugated anti–c-kit (Becton Dickinson Bioscience), phycoerythrin-conjugated anti–Thy 1 (Becton Dickinson Bioscience), and fluorescein isothiocyanate-conjugated anti-B220 antibodies (Becton Dickinson Bioscience) at the rate of 1 μg per 10^6 total cells, mixed well, and incubated in the tube for 30 to 40 minutes at 4°C. Following the incubation with the first antibody, the cells were washed twice by 0.02 mol/L phosphate-buffered saline (PBS) and centrifuged at 500*g* for 5 minutes. Labeled cells were then reacted to allophycocyanin-conjugated streptavidin (Becton Dickinson Bioscience) at the rate of 1 μg per 10^6 total cells, mixed well, and incubated in the tube for 30 to 40 minutes at 4°C. After that, these were washed out once with 0.02 mol/L PBS and centrifuged at 500*g* for 5 minutes. The labeled cells were analyzed using FACS Calibur (Becton Dickinson Bioscience).

Preparation of Liv8-positive and Liv8-negative BMCs Liv8-positive and Liv8-negative BMCs were prepared as described previously.[12] Briefly, prepared BMCs were reacted to rat anti-Liv8 immunoglobulin G (IgG) antibody at the rate of 1 μg per 10^6 total cells, mixed well, and incubated in the tube for 30 minutes at 4°C. Cells were then washed twice by 0.02 mol/L PBS and centrifuged at 500*g* for 5 minutes. Cells were labeled with rat anti-Liv8 IgG antibody by reacting with goat anti-rat IgG MicroBeads (Miltenyi Biotec GmbH, Bergisch Gladbach, Germany) at the rate of 20 μL per 10^7 total cells, mixed well, and incubated for 20 minutes at 4°C. Labeled cells were washed once by 0.02 mol/L PBS and centrifuged at 500*g* for 5 minutes. These cells were separated into Liv8-positive cells or Liv8-negative cells by the autoMACS magnetic cell sorting system (Miltenyi Biotec GmbH) for 10 minutes per tube.

Tissue Preparation and Immunohistochemistry. The liver was perfused via the heart with 4% paraformaldehyde to flush out blood cells and incubated with 4% paraformaldehyde overnight. Tissues were then soaked in 30% sucrose for 3 days. Tissues were frozen with liquid nitrogen to prepare for sectioning with a cryostat for immunohistochemistry.

Cells expressing GFP and matrix metalloproteinase (MMP)-9 (or α-smooth muscle actin) were analyzed by both fluorescent microscopy and conventional immunohistochemistry using anti-GFP, anti–MMP-9 (Santa Cruz Biotechnology, Santa Cruz, CA), and anti–α-smooth muscle actin antibodies (Sigma-Aldrich, St. Louis, MO). Tissues were soaked in 0.3% Triton X-100 with 0.05% normal goat serum (NGS) (Chemicon, Temecula, CA) or normal rabbit serum (NRS) (Chemicon) in PBS overnight. The next day, the tissues were put in 500 mL of 10% NGS or NRS in 0.3% Triton X-100 of PBS for 2 hours, then washed with 0.3% Triton X-100 with 0.05% NGS or NRS in PBS for 10 minutes. We soaked the tissues in 1.5% H_2O_2 in 50% methanol with distilled water for 2 hours. The tissues were then washed in 0.3% Triton X-100 with 0.05% NGS or NRS in PBS. Sections were incubated with anti-GFP and anti–MMP-9 (ICN Pharmaceuticals Inc., Kanagawa, Japan) antibodies. Anti–biotin-conjugated anti-goat IgG, anti-rabbit IgG, biotin-conjugated rabbit anti-goat IgG, and biotin-conjugated rabbit anti-mouse IgG were purchased from Dako Japan (Kyoto, Japan) and used as the secondary antibodies. PAP-goat (B0157), PAP-mouse (B0650), and PAP-rabbit (Z0113) polyclonal antibodies (Dako Japan) were used as third antibodies.

For fluorescent immunohistochemistry, we used Alexa Fluor R 488 and 568 donkey anti–goat- or anti–rabbit-

or anti–mouse-IgG (H + L)-conjugated antibodies (Molecular Probe Inc., Eugene, OR) as second antibodies.

For the evaluation of fibrosis, picro-sirius red staining was performed using 0.1% picro-sirius red solution as previously described.[14]

Quantitative Analysis of Liver Fibrosis. We quantified the liver fibrosis area with picro-sirius red staining using an Olympus Provis microscope equipped with a CCD camera (Tokyo, Japan), as described previously.[15] Briefly, the red area, considered the fibrotic area, was assessed by computer-assisted image analysis with MetaMorph software (Universal Imaging Corporation, Downingtown, PA) at a magnification of ×40. The mean value of 6 randomly selected areas per sample was used as the expressed percent area of fibrosis.

Microarray Analysis. Microarray analysis was performed as described previously.[16]

Briefly, total RNA of liver was isolated using the Atlas Pure Total RNA labeling system (Clontech Laboratories, Inc.) from mice 1 week after BMC transplantation (n = 3) or from mice treated with CCl_4 for 5 weeks (n = 3) according to the manufacturer's recommendations. Differential hybridization analysis was done using an Atlas Mouse complementary DNA expression array (BD Bioscience Clontech, Tokyo, Japan). Complementary DNA probe preparation and hybridization were done according to the manufacturer's recommendations. The array results were scanned with a Strom 840 PhosphoImager (Molecular Dynamics, Sunnyvale, CA) and analyzed with Atlas Image software (BD Bioscience Clontech). The results show the mean values of 3 mice in each group.

Hydroxyproline Content. Hydroxyproline content was determined by a modification of Kivirikko's method, as previously reported.[17] Briefly, liver specimens were weighed, and 20 mg of the freeze-dried sample was hydrolyzed in 6 mol/L HCl at 110°C in an autoclave at a pressure of 1.2 kg force/cm^2 for 24 hours. After centrifugation at 2,000 rpm at a temperature of 4°C for 5 minutes, 2 mL of supernatant was mixed with 50 mL of 1% phenolphthalein and 8 N KOH to obtain a total volume of 5 mL of liquid at pH of 7 to 8. Absorbance was measured at 560 nm. The hydroxyproline content of the liver was expressed as micrograms per gram of wet weight.

In Situ *Hybridization.* *In situ* hybridization was performed essentially as described previously.[18] Briefly, digoxigenin (DIG)-11-UTP–labeled single-stranded RNA probes were prepared with DIG RNA labeling mix and the corresponding T3 or T7 RNA polymerase (Boehringer Mannheim Japan, Tokyo, Japan) according to the manufacturer's instructions. The mouse MMP-9 probe was a 150–base pair fragment from the 3′ untranslated region cloned in the pBluescript (Stratagene, Tokyo, Japan) vector. *In situ* hybridization was performed on tissue sections placed on Superfrost Plus slides postfixed in 4% paraformaldehyde in PBS, rinsed in PBS containing 0.1% active diethyl pyrocarbonate, and prehybridized for 2 hours at 58°C in 50% formamide, 5 × SSC (standard saline citrate), and 40 μg of salmon-sperm DNA per milliliter. Hybridization was carried out at 58°C for 16 hours in a humid chamber with 400 ng of DIG-labeled probe per milliliter diluted in the same solution used for prehybridization. After hybridization, the sections were successively washed in 2 × SSC at room temperature for 30 minutes, 2 × SSC for 1 hour at 65°C, and 0.1 × SSC at 65°C for 1 hour. For the reaction of anti-DIG antibodies, slides were preincubated in buffer A (100 mmol/L Tris, 150 mmol/L NaCl [pH 7.5]), and then with an alkaline phosphatase-coupled anti-DIG antibody (Boehringer Mannheim Japan) diluted 1:5,000 in buffer A containing 0.5% Boehringer blocking reagent for 2 hours at room temperature. The slides were washed in buffer A and then preincubated in buffer C (100 mmol/L Tris, 50 mmol/L $MgCl_2$ [pH 9.5]). Alkaline phosphatase was then revealed as described for 16 to 24 hours at room temperature. The enzymatic reaction was stopped with Tris-ethylenediaminetetraacetic acid (EDTA) for 15 minutes. The slides were rinsed in water for several hours and then dried, cleared in xylene, and mounted directly.

In Situ *Zymography.* *In situ* zymography was performed as described.[19]

The fresh specimens of CCl_4 treated with BMC-transplanted liver tissues (1 week after BMC transplantation) were embedded without fixation in Tissue-Tek optimal cutting temperature compound (Miles, Elkhart, IN). Serial frozen sections were made using a cryostat (MicroM, Walldorf, Germany) and mounted on gelatin films that were coated with 7% gelatin solution (Fuji Photo Film, Tokyo, Japan). The films with sections were incubated for 24 hours at 37°C in a moisture chamber and stained with 1.0% amido black 10B. The gelatin in contact with the proteolytic areas of the sections was digested, and thus zones of enzymic activity were indicated by negative staining. The digested areas in the sections were compared with serial sections stained with hematoxylin-eosin. As a control, liver tissues treated with CCl_4 alone (5 weeks) were used, and the frozen sections were treated in a manner similar to that already described.

Statistical Analysis. Results are presented as the mean ± SD. Differences between groups were analyzed by 1-way ANOVA.

The survival rate was examined using the Breslow-Gehan-Wilcoxon test.

Ethical Considerations. This experiment was reviewed by the Committee of Animal Experiment Ethics at

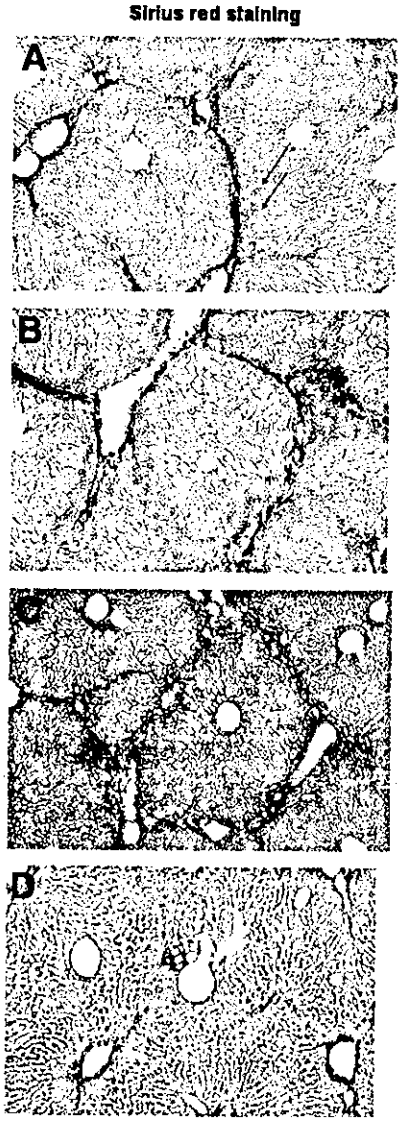

Fig. 1. Photomicrographs of liver sections stained with sirius red from mice after BMC transplantation with continuous CCl_4 treatment. Six-week-old C57BL6 mice were treated with CCl_4 twice a week for 4 weeks. Then, 1×10^5 GFP-positive BMCs were injected through the tail vein. Mice continued to be treated with CCl_4. After (A) 1, (B) 2, (C) 3, and (D) 4 weeks, mice were killed to assess the extent of liver fibrosis. (Original magnification, ×100.)

the Yamaguchi University School of Medicine and was carried out under the guidelines for animal experiments at Yamaguchi University School of Medicine (no. 105).

Results

Five weeks after CCl_4 injection, liver fibrosis was already seen (Supplementary Fig. 1A). One week after BMC transplantation (5 weeks after CCl_4 injection), BMCs were seen along with the fibers recognized by light red staining (black arrows), different from hepatocytes (Fig. 1A) with sirius red staining. More BMCs were seen after 2 weeks (Figs. 1B and 2A,C) and 3 weeks (Figs. 1C and 2B,D), and large spheroid-shaped cells (blue arrows) and small cells (green arrows) (Fig. 2B) were found in the area presumably occupied by fibers (Fig. 2D), shown by sirius red and GFP staining.

Surprisingly, 4 weeks later, the BMC-transplanted liver clearly showed reduction of liver fibrosis (Fig. 1D) compared with the liver treated with CCl_4 alone at 8 weeks (Supplementary Fig. 1D), although CCl_4 was injected throughout the experimental period. Quantitative image analysis of liver fibrosis indicated that the percent area of liver fibrosis at 1 week after BMC transplantation was 5.36% ± 0.90%, but at 4 weeks after transplantation it was significantly decreased to 4.16% ± 0.53% ($P < .001$, n = 8 each; Fig. 3).

Treatment with CCl_4 alone for 8 weeks showed an increased hydroxyproline content of 630 ± 93 μg/wet g liver (Table 1). BMC transplantation significantly reduced this to 392 ± 59 μg/wet g liver 4 weeks later ($P < .01$, n = 8 each). This hydroxyproline content was significantly reduced even compared with that of 1 week after BMC transplantation (494 ± 74 μg/wet g liver, $P < .05$).

The mouse fetal liver at E11.5 functions as a definitive hematopoietic organ, and Liv8-positive cells of the fetal liver at E11.5 include c-kit–positive immature hematopoietic cells and CD45-positive lymphoid cells. These results indicate that almost all Liv8-positive cells are of hematopoietic origin (Supplementary Fig. 2).

In addition, all c-kit–positive mouse adult BMCs belong to the Liv8-positive fraction, and Liv8-positive BMCs include almost all of the CD45- and Thy-1–positive BMCs, in addition to B220, a marker of B lymphocytes (Fig. 4).

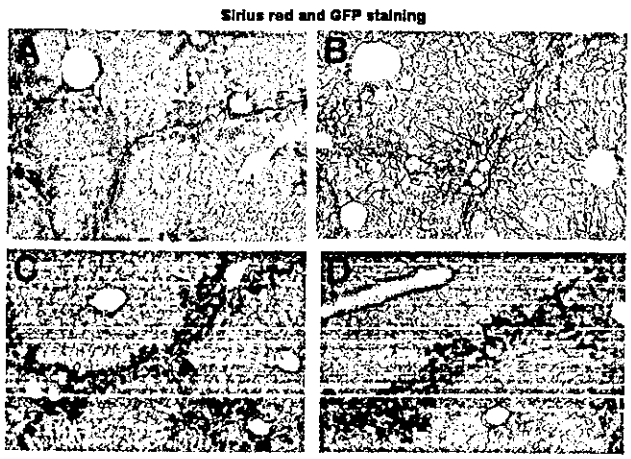

Fig. 2. Photomicrographs of liver sections stained with sirius red or sirius red and GFP from a mouse (A, C) 2 weeks and (B, D) 3 weeks after BMC transplantation. (Original magnification, [A] ×200; [B] ×200; [C] ×200; [D] ×200.)

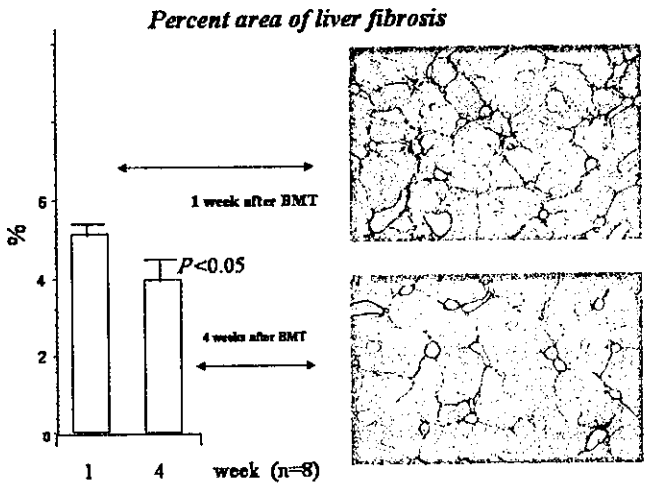

Fig. 3. Quantitative analysis of liver fibrosis after bone marrow cell transplantation (BMT). Percent area of liver fibrosis was calculated using sirius red staining as described in Materials and Methods. Results are expressed as mean ± SD of 8 samples. (Original magnification, ×40.)

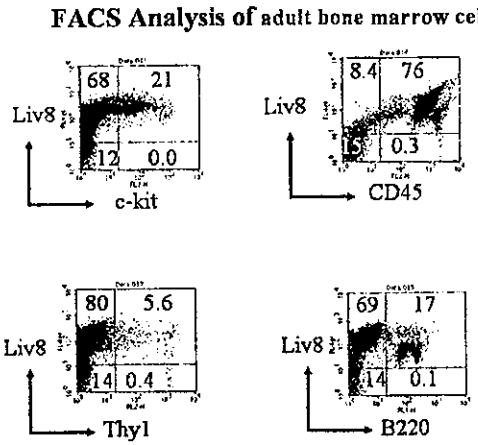

Fig. 4. Expression of Liv8, c-kit, CD45, Thy 1, and B220 in adult BMCs.

These results strongly suggest that Liv8-positive cells include both immature and mature hematopoietic cells.

Liv8-negative BMCs significantly reduced liver fibrosis compared with that of the liver treated with CCl4 alone for 8 weeks, although Liv8-positive BMCs had no effect on liver fibrosis (Table 2).

Microarray analysis of the liver 1 week after BMC transplantation indicated increased expression of MMP-2, MMP-9 and MMP-14 with decreased expression of tissue inhibitor of metalloproteinase-3 (TIMP-3) compared with that of the liver treated with CCl_4 alone for 5 weeks (Table 3). Because the expression of MMP-9 was marked, we investigated it in this model.

Immunohistochemistry of MMP-9 showed localization of these cells similar to that of transplanted BMCs (Fig. 5A). However, the liver treated with CCl_4 alone showed only a few MMP-9–positive nonparenchymal cells (black arrows, Fig. 5B).

The expression of MMP-9 with *in situ* hybridization coincided with the immunohistochemical staining of MMP-9 (Fig. 5C).

Table 1. Hydroxyproline Content

Treatment (No. of Mice)	Hydroxyproline (μg/g Liver)
CCl_4, 5 wk (8)	464 ± 93
CCl_4, 8 wk (8)	630 ± 93
CCl_4/BMT, 5 wk (8)	494 ± 74
CCl_4/BMT, 8 wk (8)	392 ± 59*†

NOTE. Mice were treated with CCl_4 for 4 weeks; then, 1 week or 4 weeks after bone marrow cell transplantation (BMT) or saline injection with CCl_4 treatment, they were killed to measure liver hydroxyproline content. Results are typical of 1 of 3 independent experiments.

*$P < .01$ vs. CCl_4 (8 weeks).

†$P < .05$ vs. CCl_4/BMT (5 weeks).

Although double fluorescent-positive cells were not seen in the liver treated with CCl_4 alone (Fig. 6A), double-positive yellow-colored cells (black arrows) were seen in the BMC-transplanted liver (Fig. 6B). With high magnification, double fluorescent immunohistochemistry showed the expression of MMP-9 (red) on the GFP-positive (green) cell surface (Fig. 6C).

A double fluorescent (anti-GFP with green color and anti–α-smooth muscle actin with red color) study indicated that a fine network pattern of stellate cells (red) existed in the liver treated with CCl_4 alone for 5 weeks (Fig. 7A). Conversely, GFP-positive green-colored cells (green arrow) were seen with a reduced fine network pattern (red arrow) in the liver 1 week after BMC transplantation (Fig. 7B). Double fluorescent-positive yellow-colored cells (yellow arrow), presumably stellate cells, were then seen without the fine network pattern (red arrow) in the liver 2 weeks after BMC transplantation (Fig. 7C). The shape of these cells was different from other GFP-positive cells, and the number of the double-positive cells was very small.

Next, we examined the direct activity of MMP-9 using *in situ* zymography. Film *in situ* zymographic analysis revealed strong gelatinolytic activity in the periportal area

Table 2. Hydroxyproline Content

Treatment (No. of mice)	Hydroxyproline (μg/g Liver)
CCl_4 (8)	687 ± 102
CCl_4/Liv8-positive (8)	638 ± 94
CCl_4/Liv8-negative (8)	415 ± 77*

NOTE. Mice were treated with CCl_4 for 4 weeks followed by transplantation with Liv8-positive or Liv8-negative BMCs or saline. After 4 weeks of CCl_4 treatment (total 8 weeks), mice were killed to measure liver hydroxyproline content. Results are typical of 1 of 3 independent experiments.

*$P < .01$ vs. CCl_4.